what is going on. For those boules containing small amounts of cobalt the oxygen treatment is, as expected, too oxidizing and there is evidence for a small amount of Fe_2O_3 formation. The CoO is clearly visible as a second phase in metallographic specimens of sections of boules as grown containing more cobalt than expressed by the ratio 0.4, Fig. 3(a). Metallographically prepared sections of these boules after the heat treatment in oxygen show large sections of single phase, single crystal [Fig. 3(b)]. These regions are shown to be single crystal by their Laue patterns.

Regardless of composition, all boules as grown were electrically *n* type. Following the heat treatment in oxygen those crystals of Co/Fe composition less than 0.5 remained *n* type, but those for which Co/Fe is greater than 0.5 converted to *p* type in agreement with the results reported by Jonker.[6]

From the reported investigations it appears that single-crystal cobalt ferrites can be prepared from two-phase material if the phases are grown coherent in structure and if crystal preparation is followed by an oxidizing (or reducing) procedure performed at a high enough temperature to permit diffusion. This suggests that the problem of nonuniformity of composition with respect to Co:Fe as a function of length of the boules due to CoO enrichment from the melt into the solid during growth might be taken care of by a high temperature oxidation of longer duration than used in these studies. Uniformity of metal ion distribution may also be achieved, in principle, by using a zone leveling procedure for crystal growth. Control of the vacancy concentration requires the use of the known appropriate temperature-oxidation conditions for the particular composition of cobalt ferrite prepared.

It would appear that the observations reported may be applied generally to the preparation of crystalline oxides grown from metals in which the atmosphere employed causes a dissociation of the solid. The requirement for the possibility of recovering single-phase single crystal is that the phases grown from the melt are coherent and oriented with respect to the oxygen lattice in the grown crystal and that conditions for an anneal after growth permit diffusion of the metal ions in the solid to the final phase desired.

This work is abstracted from a study on ferrites performed in cooperation with G. A. Slack and W. E. Engeler. I wish to acknowledge the work of P. Friguletto in forming, preparing, and annealing crystals.

JOURNAL OF APPLIED PHYSICS VOLUME 33, NUMBER 9 SEPTEMBER 1962

Electrical Properties of Single Crystals of Indium Oxide

R. L. WEIHER
Central Research Laboratories, Minnesota Mining & Manufacturing Company, St. Paul, Minnesota
(Received February 23, 1962)

An investigation of electrical properties of indium oxide single crystals has been made. Indium oxide has been found to be a *n*-type excess semiconductor over a wide temperature range. The electrical conductivity at room temperature is of the order of 10 Ω cm^{-1} and the mobility is approximately 160 cm^2 V-sec^{-1}. The temperature dependence of the mobility has been quantitatively interpreted in terms of lattice and ionized impurity scattering. The donor ionization energy has been found to decrease with increasing impurity concentrations. High "apparent intrinsic" conductivity with an activation energy of 1.55 eV has been observed at elevated temperatures.

I. INTRODUCTION

ONE of the first investigations of indium oxide (In_2O_3) as a semiconductor was made by Rupprecht[1] on thin vapor-coated films. Because of the polycrystalline nature of the films, most of the phenomena he observed can be attributed to surface and barrier effects. Although studies as the above contribute much to the over-all knowledge of a material, studies of single crystals are required to observe true bulk effects.

It is the purpose of this paper to present an investigation of some of the electrical properties of single crystals of indium oxide recently grown in this laboratory. The investigation consists of low temperature conductivity and Hall effect measurements along with conductivity measurements at elevated temperatures. Analysis of the presented data reveals mechanisms of conduction common among the many semiconductors previously investigated.

II. MATERIAL PREPARATION

Single crystals of indium oxide were grown from the vapor phase of indium metal and ambient oxygen. Approximately equal amounts of carbon and indium metal were mixed in a porcelain crucible, loosely covered, and heated in a furnace at 1000°C for 24 h. Pale yellow, needle-shaped crystals approximately 0.5×0.5×5.0 mm in size grew on the walls and cover of the crucible. The crystals were identified as In_2O_3 by x-ray diffraction. Square and hexagonal cross sections were obtained corresponding to growth in the [100] and

[1] G. Rupprecht, Z. Physik **139**, 504 (1954).

[111] crystal directions, respectively. The crystal structure of indium oxide is body-centered cubic. The crystals of growth in the [111] direction were used for the electrical measurements discussed herein. Spectrochemical analysis indicated that silicon and molybdenum were the only impurities present in concentrations slightly greater than one part in 10^6. However, because of the small quantity of crystals available the absolute value of impurity content could not be ascertained for the four crystals discussed herein. Electrical measurements indicate impurity concentrations of the order of 10^{18} per cc which is much greater than the estimate from spectrochemical analysis. It is on this basis that we conclude that the electrically active impurities are probably a stoichiometric excess of indium or effective imperfections such as oxygen vacancies.

III. LOW-TEMPERATURE ELECTRICAL MEASUREMENTS

A. Experimental Apparatus

The sample holder used for electrical conductivity and Hall effect measurements at low temperatures is shown in Fig. 1. The top probe assembly is spring loaded to simplify crystal removal, to hold the crystal in place, and to maintain sufficient pressure for probe contacts. The current leads were attached to the ends of the crystals by electrolytically reducing the ends of the crystals to indium metal, tying No. 38 copper wire over the indium metal and then painting over the indium-copper contacts with silver paste. This method gave strong, low resistance contacts.

The crystal holder was enclosed in a copper box to maintain a uniform temperature and act as a radiation shield. The complete assembly of apparatus is shown in Fig. 2. The entire apparatus was maintained in a vacuum of approximately 0.5 μ of mercury. The cooling of the sample was accomplished by immersing the cooling substage in liquid nitrogen until the desired temperature was obtained. The magnet for Hall measurements was raised and lowered by a pulley system controlled outside the vacuum.

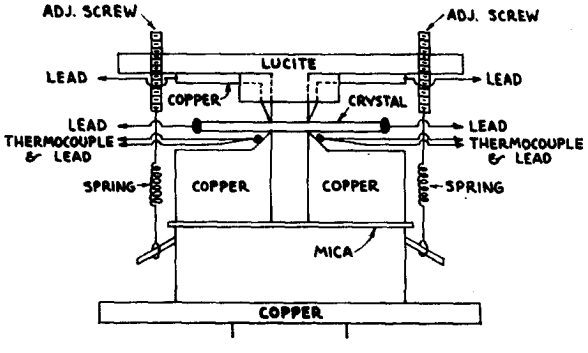

FIG. 1. Low-temperature sample holder.

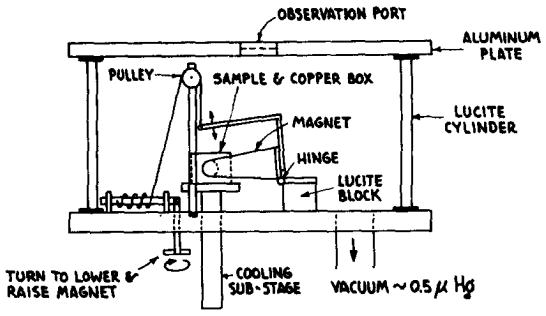

FIG. 2. Complete low-temperature experimental apparatus.

A Keithley 200B electrometer was used to measure the potential drop across the conductivity probes and a Weston 430 ammeter was used to measure the current. The Hall voltage was measured with a Cary 31 vibrating reed electrometer. The temperature was measured with copper-Constantan thermocouples and a Leeds and Northrup potentiometer.

B. Electrical Conductivity

The largest variation in electrical conductivity at room temperature for the crystals as-grown was from approximately 5 to 50 $\Omega\ cm^{-1}$. Figure 3 depicts the conductivity of four such crystals as a function of temperature from room temperature to 90°K. Four approximately parallel curves are obtained with maxima at about −100°C and no specific activation energy in this temperature range. The curves reflect the fast decreas-

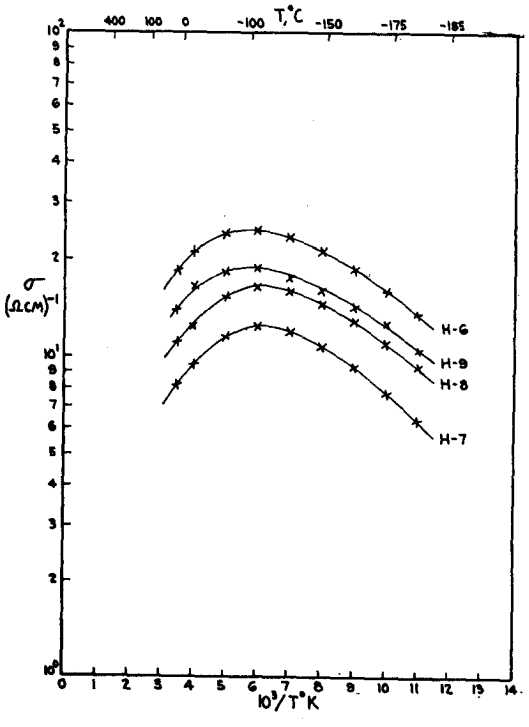

FIG. 3. Electrical conductivity vs temperature for four single crystals of indium oxide.

ing mobility in the near "saturation" range at higher temperatures and the changing number of ionized donors in the lower temperature range.

C. Carrier Concentration Analysis

Hall measurements on the single crystals indicate n-type conductivity. It will be assumed that there is no impurity band conduction so that all the conduction is in the conduction band. If one assumes single band conduction, spherical energy surfaces, noninteracting carriers, etc., one can show that the Hall mobility differs from the microscopic mobility by some factor which depends upon the type of scattering mechanism involved. Because the validity of the above assumptions, along with other assumptions required for a direct conversion from Hall mobility to microscopic mobility, is not known, the more accepted conversion $(3\pi/8)$ will be used; that is, the carrier concentration was calculated from

$$n=(3\pi/8)(\sigma/e\mu_H). \quad (1)$$

Shown in Fig. 4 are four curves of carrier concentration as a function of temperature calculated from Eq. (1). The donor ionization energies cannot be obtained directly from these curves for two reasons: (1) Because of the weak temperature dependence of the carrier concentrations, the density-of-states (N_c) cannot be considered constant (2), degeneracy of the donor level must be considered. The donor ionization energy can, however, be determined with the type of analysis

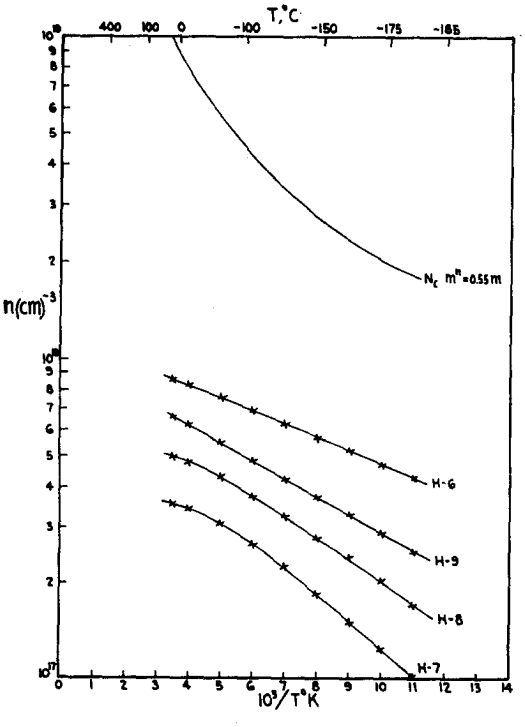

FIG. 4. Carrier concentrations vs temperature for four single crystals of indium oxide.

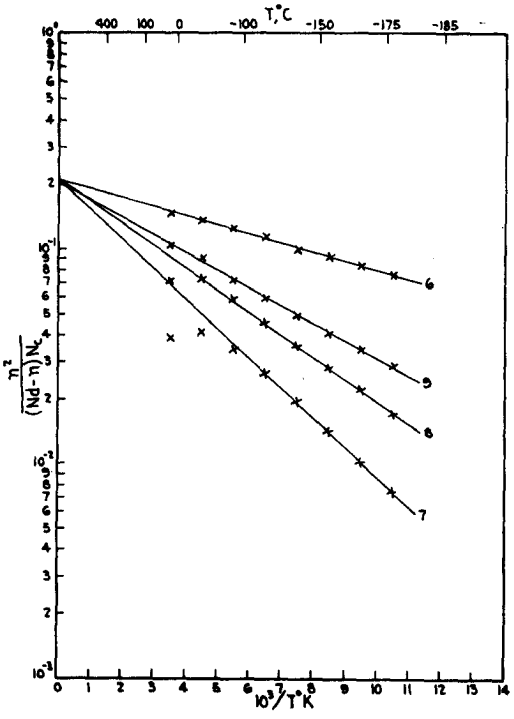

FIG. 5. Determinations of donor ionization energies for four single crystals of indium oxide.

presented by Hutson[2] in which degeneracy of the donor level was considered. Assuming only one major donor level (ϵ_d) in the vicinity of the Fermi level (ϵ_f) and degenerate statistics for this donor level, the number of un-ionized donors (n_d) can be written as

$$n_d=N_d/[1+g^{-1}\exp(\epsilon_d-\epsilon_f)/kT], \quad (2)$$

where $N_d=n_d+n$. The factor g is the spin degeneracy of the donor states. If nondegeneracy is assumed for the carrier population in the conduction band, the concentration of conduction band electrons can be expressed by,

$$n=N_c\exp(\epsilon_f-\epsilon_c)/kT, \quad (3)$$

where $N_c=2(2\pi m^n kT/h^2)^{\frac{3}{2}}$ and m^n=density-of-states effective mass. The value of m^n, which determines the validity of the use of Eq. (3) in this case, was approximated by the conjunctive use of Hall and thermoelectric power measurements to be $\sim 0.55m$, where m is the free electron mass. The effective density-of-states using $m^n=0.55m$ is depicted by the upper curve of Fig. 4 from which values of N_c/n tend to validate Eq. (3). Eliminating n_d and ϵ_f from Eqs. (2) and (3), one obtains the expression

$$n^2/(N_d-n)B_c=(m^n/m)^{\frac{3}{2}}g^{-1}\exp(\epsilon_d-\epsilon_c)/kT, \quad (4)$$

where B_c is the effective density-of-states for $m^n=m$. Therefore, if one plots the logarithm of the left-hand side of Eq. (4) vs $1/T°K$, one should obtain a straight

[2] A. R. Hutson, Phys. Rev. **108**, 222 (1957).

line with a slope of $(\epsilon_d-\epsilon_c)/k$ with an intercept, as $1/T\rightarrow 0$, equal to $(m^n/m)^{\frac{3}{2}}g^{-1}$.

The results of this treatment on the four single crystals of indium oxide using Eq. (4) are depicted in Fig. 5. The only parameter in $n^2/(N_d-n)B_c$ not directly known is N_d, which was arbitrarily chosen to give the best straight line fit at the lower temperatures. At higher temperatures, when n becomes comparable in magnitude to N_d, small experimental errors in n have a pronounced effect and values may deviate slightly from a straight line. Attempts at introducing slight compensation resulted in curves which deviated from a straight line greater than if one assumes no compensation. A summary of the values obtained for N_d and $\epsilon_d-\epsilon_c$ by this analysis is given in Table I.

The dependence of the ionization energy on the donor concentration shown in Table I is an effect common with semiconductors. When impurities are present in sufficient quantities so that there are electrostatic interactions between centers and other crystal imperfections, the simple hydrogen-like model is not realized and the ionization energy decreases with increasing impurity concentration. This decrease in ionization energy with increasing impurity concentration is usually explained as a broadening of the impurity level due to overlap of wave functions of the hydrogen-like centers.

Pearson and Bardeen[3] have suggested a model for the decrease in ionization energy with increasing donor concentrations by considering the electrostatic attraction of donors for an electron which has escaped from its own donor. This consideration yields the expression

$$\epsilon_d=\epsilon_{d0}-\alpha N_d^{\frac{1}{3}}, \tag{5}$$

where ϵ_d is the donor ionization energy for a given concentration of donors, ϵ_{d0} is the donor ionization energy when the number of donors approaches zero, α is a constant, and N_d is the number of donors. The data in Table I plotted as shown in Fig. 6 indicate good agreement with this model, at least in our very limited range of donor concentrations. The donor ionization energy as a function of donor concentration shown in Fig. 6 is then calculated to be,

$$\epsilon_d=0.093\text{ eV}-8.15\times10^{-8}N_d^{\frac{1}{3}}\text{ eV}. \tag{6}$$

These data predict that the donor ionization energy should effectively go to zero for a donor concentration of 1.48×10^{18} cm^{-3}.

TABLE I. Summary of donor ionization energies and donor concentrations for four single crystals of indium oxide.

Crystal No.	$(\epsilon_d-\epsilon_c)$ eV	N_d cm^{-3}
H-6	0.0085	1.09×10^{18}
H-9	0.0166	8.40×10^{17}
H-8	0.0210	6.50×10^{17}
H-7	0.0280	4.95×10^{17}

[3] G. L. Pearson and J. Bardeen, Phys. Rev. 75, 865 (1949).

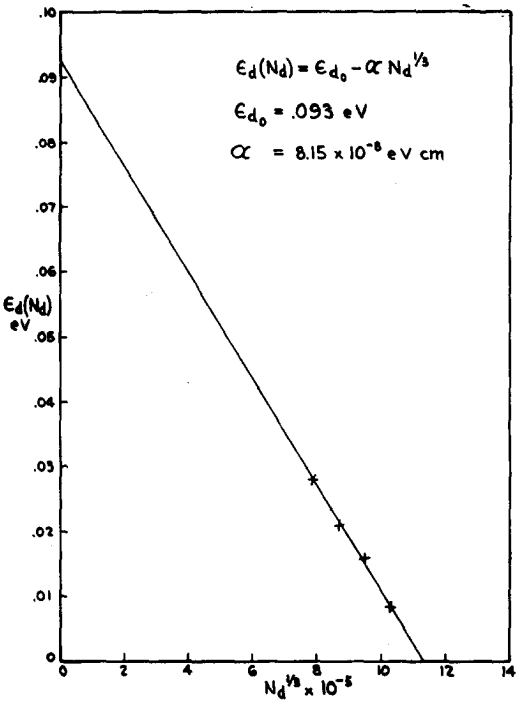

FIG. 6. Donor ionization energies vs impurity concentrations.

It is seen in Fig. 5 that the quantity $(m^n/m)^{\frac{3}{2}}g^{-1}$ given by the intercept is equal to 0.205. If one uses the approximate value of effective mass $(m^n=0.55m)$, previously discussed, a value of 2.0 is obtained for the g factor. This suggests that the impurity level can be described as a simple donor state with one electron of either spin. This is, however, consistent with assumptions implicit in Eq. (2) for which the excited states of the impurities were assumed negligible. If one is to consider the excited states, Eq. (2) should be rewritten as given by Shifrin,[4]

$$n_d=N_d\sum_{r=0}^{\infty}[1+g_r^{-1}\exp(\epsilon_r-\epsilon_f)/kT]^{-1}, \tag{7}$$

where ϵ_r and g_r are the energy and degeneracy of the rth state, respectively. The assumption in Eq. (2) is, therefore, to neglect the terms other than the $r=0$ term for which $g=2$ and $\epsilon_r=\epsilon_d$ for a simple donor with one electron with either spin.

D. Mobility Analysis

The polarity of the Hall potential indicates n-type conductivity, so the mobility under consideration in this section is for the electrons in the conduction band. The marks in Fig. 7 represent the experimental Hall mobilities as a function of temperature, from room temperature to 90°K, for four single crystals. Included in Fig. 7 are four solid lines represented by the expres-

[4] K. S. Shifrin, Zhur. Tekh. Fiz. 14, 43 (1944).

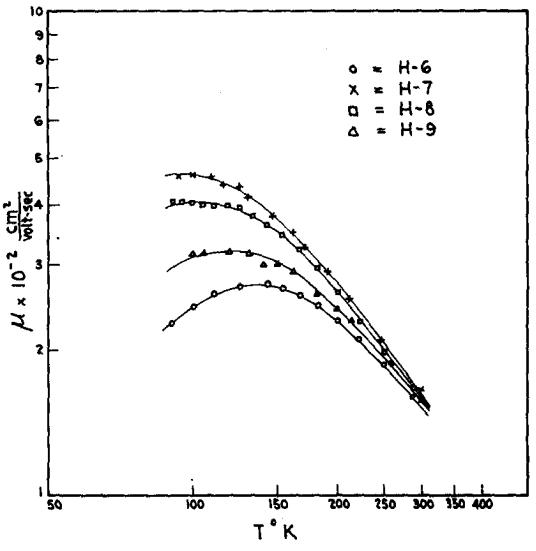

FIG. 7. Carrier mobilities vs temperature for four single crystals of indium oxide.

sion,

$$\mu_H = ABT^{\frac{3}{2}}/(A+BT^3), \tag{8}$$

where A is a constant for all curves, and B is a constant for a given curve but varies with the particular curve. It is seen that the solid lines represented by Eq. (8) fit the experimental mobility data extremely well.

Equation (8) can be interpreted as a combination of acoustical mode lattice scattering and ionized impurity scattering if one assumes that the total resistivity (ρ) is simply a sum of the resistivities due the various scattering mechanisms so that,

$$\rho = \rho_L + \rho_i, \tag{9}$$

or,

$$1/\mu = (1/\mu_L) + (1/\mu_i). \tag{10}$$

Bardeen and Shockley[5] have shown that for acoustical mode lattice scattering, the mobility can be expressed as,

$$\mu_L = \frac{(8\pi)^{\frac{1}{2}}\hbar^4 c_{22}}{3\epsilon_{1n}^2 (m^m)^{\frac{3}{2}}(kT)^{\frac{3}{2}}}, \tag{11}$$

where c_{22} is the average longitudinal elastic constant and ϵ_{1n} is the shift of the edge of the band per unit dilation. c_{22} and ϵ_{1n} are usually considered to be temperature independent, thus

$$\mu_L = AT^{-\frac{3}{2}}, \tag{12}$$

where A is a constant.

Conwell and Weisskopf[6] have shown that for ionized impurity scattering, the mobility can be expressed as,

$$\mu_i = \frac{2^{7/2}K^2(kT)^{\frac{3}{2}}}{\pi^{\frac{3}{2}}(m^m)^{\frac{1}{2}}e^3 N_i} \times \frac{1}{\ln[1+(3KkT/e^2 N_i^{\frac{1}{3}})^2]}, \tag{13}$$

where N_i is the concentration of impurities and K is the dielectric constant. The logarithmic term is usually considered to be a slow varying function of temperature and therefore the mobility due to ionized impurities can be approximated as,

$$\mu_i = BT^{\frac{3}{2}}, \tag{14}$$

where B is a constant. Summing the reciprocals of Eqs. (12) and (14), as previously assumed, yields Eq. (8) for which the experimental mobilities fit.

The experimental value of the constant A in Eq. (12) was found to be 8.52×10^5 and constant for all the crystals. It is seen from Eqs. (13) and (14) that the constant B should be approximately proportional to N_i^{-1} or the product BN_i should be approximately a constant. The values obtained experimentally, shown in Table II, show reasonable agreement between theory and experiment.

The apparent agreement between experiment and theory is probably better than should be expected from the approximations and assumptions implicit in Eqs. (1), (10), and (14). For instance, Conwell[7] has shown that simply summing the reciprocals of the individual mobilities [Eq. (10)] is not accurate since the relaxation times for the various scattering mechanisms are dependent upon energy in different ways. It is therefore concluded that although Eq. (8) fits the experimental data extremely well, the interpretation of Eq. (8) could be somewhat in error.

TABLE II. Summary of the experimentally determined constants of Eqs. (12) and (14).

Crystal No.	N_i cm^{-3}	B	BN_i	A
H-6	1.09×10^{18}	0.344	3.8×10^{17}	8.52×10^5
H-7	4.95×10^{17}	1.000	4.9×10^{17}	8.52×10^5
H-8	6.50×10^{17}	0.758	4.9×10^{17}	8.52×10^5
H-9	8.40×10^{17}	0.480	4.0×10^{17}	8.52×10^5

ELECTRICAL CONDUCTIVITY AT ELEVATED TEMPERATURES

Measurements of the electrical conductivity of the single crystals were extended from room temperature to 1500°C using a spring loaded, four-probe apparatus similar to that shown in Fig. 1. No Hall measurements were made at the elevated temperatures. The measurements were made in a normal atmosphere ($P_{O_2}\sim0.2$ atm) in which no detectable sublimation took place.

A typical curve of the electrical conductivity as a function of temperature, from approximately 1700° to 90°K, is shown in Fig. 8. The lower portion of the temperature range was discussed in Sec. IIIB. What is of greater interest here, is the dramatic increase in

[5] J. Bardeen and W. Shockley, Phys. Rev. **80**, 72 (1950).

[6] E. Conwell and V. Weisskopf, Phys. Rev. **77**, 388 (1950).

[7] E. Conwell, Proc. IRE **40**, 1327 (1952).

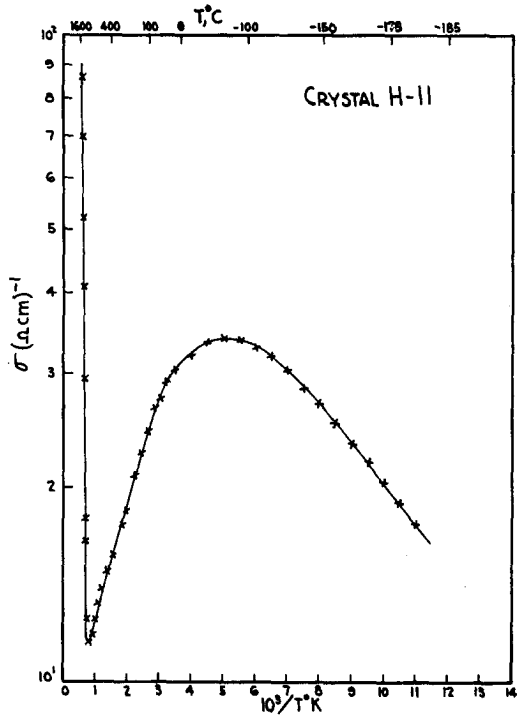

FIG. 8. Electrical conductivity vs temperature from 90° to 1700°K.

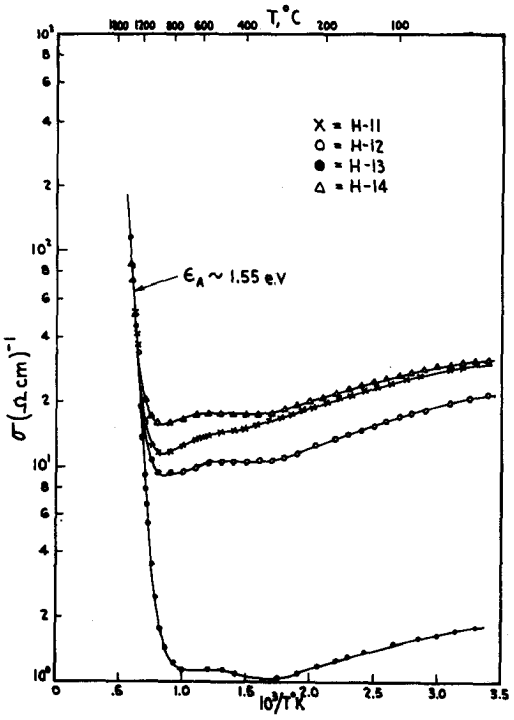

FIG. 9. Electrical conductivity vs temperature from room temperature to 1700°K for four single crystals of indium oxide.

conductivity at high temperatures, which resembles intrinsic conductivity. The electrical conductivity of various crystals coincide at high temperatures with a common "activation energy" ($\epsilon_A \sim 1.55$ eV) as shown in Fig. 9. The electrical conductivity can thus be represented, in this temperature range, as

$$\sigma = \sigma_0 \exp -1.55/kT. \tag{15}$$

It should probably be mentioned that crystal HZ-13 of Fig. 9 is of lower conductivity due to the addition of a small amount of zinc added during growth.

The interpretation of the "apparent intrinsic" conductivity is difficult at this time because at least two different mechanisms are capable of giving plausible explanations: (1) Band-to-band transitions, and (2) dissociation of the compound. If one considers band-to-band transitions with the assumptions that the density-of-states is proportional to $T^{\frac{3}{2}}$, the mobility is proportional to $T^{-\frac{3}{2}}$, and that the band gap varies linearly with temperature, one can express the conductivity as,

$$\sigma = \text{const} \exp \epsilon_{g0}/2kT, \tag{16}$$

where ϵ_{g0} is the band gap at absolute zero. This consideration yields a band gap of 3.1 eV for indium oxide which is in close agreement with optical determinations. Rupprecht[1] has reported the value of 3.5 eV for the band gap of indium oxide as determined from optical transmission measurements on thin vapor coated films. However, preliminary optical measurements being conducted in this laboratory on thin crystal plates indicate a band gap nearer 3.1 eV.

Although the above consideration gives quite a convincing argument for band-to-band transitions, other facts remain which indicate that the "apparent intrinsic" conductivity is due to a dissociation of the compound. Electrical measurements on thin films of indium oxide by Rupprecht[1] show that at a constant temperature, above 500°C, the conductivity is dependent on oxygen pressure ($\sigma \propto P_{O_2}^{-0.19}$). Rupprecht suggests the dissociation reaction,

$$In_2O_3 \rightleftarrows 2\,In^{+3} + 6e^- + \tfrac{3}{2}\,O_2, \tag{17}$$

which, with the aid of the law of mass action, predicts that the conductivity should be proportional to $P_{O_2}^{-0.1875}$. From the agreement between the experimental and calculated oxygen pressure dependences, it is evident that dissociation of the compound must at least be considered as a probable mechanism for the "apparent intrinsic" conductivity because the oxygen pressure dependence seems unlikely for true intrinsic conductivity.

ACKNOWLEDGMENTS

The author wishes to thank his colleagues in this laboratory, especially G. K. Lindeberg, for helpful discussions and suggestions. The author also wishes to thank B. Gale Dick of the University of Utah for his valuable consultation, especially in theory. He is also indebted to F. A. Hamm for making this work possible.